Applied Thermal Engineering 257 (2024) 124084

Contents lists available at ScienceDirect

Applied Thermal Engineering

journal homepage: www.elsevier.com/locate/apthermeng

Research Paper

Thermal resilience of buildings: The role of partition walls and slabs in the optimization of the building external envelope

Francesco Leccese [a], Giacomo Salvadori [a,*], Fabio Bisegna [b]

[a] Department of Energy, Systems, Territory and Constructions Engineering (DESTeC), University of Pisa, Pisa, Italy
[b] Department of Astronautic, Electric and Energy Engineering (DIAEE), Sapienza University, Rome, Italy

ARTICLE INFO

Keywords:
Passive behaviour
Energy performance
Building envelope
Multi-layered walls
Thermal insulation
Thermal resilience

ABSTRACT

Nowadays it is advisable for buildings to be thermally resilient, so as to passively resist to the daily external air temperature fluctuations, reducing the interventions of air conditioning systems to a minimum. The decrement factor and time lag are parameters notoriously used to evaluate the responses of the building envelope to periodic oscillations in external air temperature. However, in their traditional definition, these parameters do not consider the effects of internal elements, such as partition walls and slabs, which instead influence the passive thermal behaviour of the building. For this reason, a choice of the external wall stratigraphy, made exclusively on the basis of the traditional decrement factor and time lag, seems to be simplistic. In this paper, problems concerning the passive behaviour of buildings, in case of sinusoidal outdoor air temperature variations, are investigated. Within a lumped-capacitance scheme and using the heat transfer matrix method, the problem of the determination of a wall stratigraphy minimizing the decrement factor for given values of the overall thermal resistance and capacity, usable for the realization of both external and internal walls of a given room, is solved. After developing an analysis on the influence of the internal walls and slabs on the room thermal balance, the resistance-capacity distribution, within the external wall, minimizing the decrement factor is determined, for assigned thermal resistances and capacities of internal elements and the external wall. Results indicate that there is no resistance-capacity distribution that is absolutely better than the others, but it is dependent on the thermophysical characteristics of the internal elements. The optimized external wall stratigraphy can be composed of an even number of resistive and capacitive layers, alternating with each other, or of an odd number of layers (with one more resistive layer than the capacitive ones). Even the number of layers that makes optimized the passive behaviour of the external wall varies with the characteristics of the internal elements, the results show that already with a number of layers varying from 2 to 5 high performances can be obtained.

1. Introduction

In the last few years an ever-growing need to reduce energy consumption has occurred in order to limit the CO_2 emissions and the impact on the environment, especially for the building sector, aiming to achieve a fully decarbonised building stock by 2050 [1]. Therefore, the energy saving achievable with an accurate energy design of buildings is very relevant, for both new constructions and renovations [2,3]. In the accurate energy design of buildings, a key role is played by the building envelope, that should be thermally resilient, so as to passively resist to the daily external air temperature fluctuations, reducing the interventions of air conditioning systems [4–6]. In mild climates, a building well designed, from a thermal point of view so as to show an optimal passive behaviour, can assure an acceptable comfort level even in absence of heating/cooling plants with consequent energy saving [7,8].The aspects of greatest consideration in the design phase for an opaque building envelope with high thermal resilience are summarized below.

- With particular reference to the steady state conditions (representative, with good approximation, of winter season), the building thermal insulation of the building envelope has to be obviously high, in order to reduce energy consumption: the higher the thicknesses of the insulating layers are, the lower the heat power to be supplied by the heating plant in order to keep the rooms at the wished temperature, under steady conditions, will be [9–11].

* Corresponding author.
E-mail address: giacomo.salvadori@unipi.it (G. Salvadori).

https://doi.org/10.1016/j.applthermaleng.2024.124084
Received 12 March 2024; Received in revised form 10 July 2024; Accepted 31 July 2024
Available online 10 August 2024
1359-4311/© 2024 The Author(s). Published by Elsevier Ltd. This is an open access article under the CC BY-NC-ND license (http://creativecommons.org/licenses/by-nc-nd/4.0/).

Nomenclature

c_s	s-th layer thermal capacity per surface unit, J m^{-2} K^{-1}
c	external wall thermal capacity per surface unit, J m^{-2} K^{-1}
$C=\Sigma c_s$	total thermal capacity per surface unit, J•m^{-2}•K^{-1}
C_p	specific heat at constant pressure, J kg^{-1} K^{-1}
D=r|Λ|	dimensionless quantity
E, F, G, H	elements of the transmission matrix of external wall
e, f, g, h	elements of the transmission matrix of inner structure
I_m	imaginary part
I_0, K_0	modified Bessel functions
$j=\sqrt{-1}$	imaginary unit
k	thermal conductivity, W m^{-1} K^{-1}
P	period, s^{-1}
Q_S	specific heat flux supplied by the air-conditioning system, W m^{-2}
Q_{int}	specific heat flux overall supplied by the internal elements, W m^{-2}
q	specific heat flux, W/m^{-2}(-|-)
r	external wall thermal resistance per surface unit, m^2 K W^{-1}
r_s	s-th layers thermal resistance per surface unit, m^2 K W^{-1}
Re	real part
R	total thermal resistance, m^2 K W^{-1}
S	external wall surface, m^2
T	temperature, K
T_0	temperature of adiabatic surface for the m-th internal element, K
T_w	wall inner surface temperature, K
U	air thermal capacity per surface unit, J m^{-2} K^{-1}
x	thickness, m

Greek symbols

$\alpha_m = S_m/S$	dimensionless weight of m-th interior partition
β	thermal diffusivity, m^2 s^{-1}
$\gamma = \omega rc$	dimensionless parameter
$\zeta = T_{int}/T_{ext}$	dimensionless parameter
θ	phase of λ, degree
λ	complex admittance of inner wall, W m^{-2} K^{-1}
Λ_0	complex admittance defined, W/m^{-2}(-|-) K^{-1}
$\lambda\infty = (\omega\xi)^{0.5}$	conductance, W m^{-2} K^{-1}
Λ	complex overall admittance of the room inner walls, W m^{-2} K^{-1}
$\mu = \omega RC$	dimensionless parameter
$\nu = (2\beta/\omega)^{0.5}$	penetration depth of a thermal oscillation within a semi-infinite solid, m
$\xi = \rho C_p k$	thermal effusivity, W^2 s m^{-4} K^{-2}
ρ	density, kg m^{-3}
σ	modified dimensionless damping factor, for taking into consideration the effect of partition walls
τ	time, s
τ_R	time lag, s
$\phi_n=\|H\|^2$	relating to the structure characterized by the number n
φ	phase of Λ, degree
$\omega = 2\pi / P$	angular frequency, rad/s

Subscripts

ext	exterior
int	interior
I	resistive layer
L	capacitive layer
m	relating to the m-th

Superscripts

′	relating to adjacent room
–	(over bar) relating to a semi-wall

- With reference to the dynamic conditions (representative of the intermediate seasons and summer, with periodic fluctuation of external temperature), thermal resistance and capacity of the opaque envelope will have to be taken into careful consideration [12–14].
- The thermal behaviour of buildings under dynamic conditions is of greater scientific interest than the steady-state one and it can be investigated from two different points of view: the first concerns the interaction between the building and the heating/cooling plants [15,16]; the second concerns the building passive behaviour [17,18].

The building passive behaviour is the subject of the present study. To improve passive behaviour and hence the thermal resilience of a building, multi-layer walls are generally used, i.e. non-homogeneous walls consisting of a sequence of layers made of different materials, some with essentially resistive thermal properties (light and insulating layers), other with essentially capacitive properties (heavy and mechanically resistant layers). The sequence in which such layers are disposed within both external walls and internal elements is essential for assuring a good passive behaviour of the building [12,17].

2. Literature framework, research gap and aim of the study

The distribution of the resistive and capacitive layers of a multi-layer wall, to optimize its passive behaviour, was analysed in an analytical and numerical way in many studies in the literature. It was proposed to evaluate the passive behaviour using decrement factor and time lag, parameters currently known and also defined in the technical standards [19]. Following, a brief description of the relevant literature which constitutes the scientific basis of the present study is reported.

In 2000, Asan [20] considered 18 different configurations of an opaque envelope wall, each of which composed of the same layers of a capacitive material and a resistant material but with a different layer sequence. Considering an external temperature periodically variable, by solving the heat transfer problem with finite-difference approach and the Crank–Nicolson method, he was able to formulate some important observations on the optimization of the stratigraphy. In particular, he observed that placing half of the insulation in the mid-centre plane of the wall and the half of it in the outer surface of the wall gives very high time lags and low decrement factors. In 2006, the same author [12] extended his study focusing on determinations of time lags and decrement factors of twenty-six different common building materials with various thickness.

In 2011, Osel [21] used an implicit finite difference method to solve the transient heat conduction problem in multi-layer walls, in order to determine the thermal performance and optimum insulation thicknesses of building walls, constructed of five different structure materials and two different insulation materials. In 2014, in subsequent study with the same approach, Ozel [22] also dealt with the evaluation of the decrement factor and time lag of different opaque envelope walls. analysing three different walls, composed of the same thickness of insulating material and capacitive material (brick), as well as plaster. The walls were differentiated by the different layer sequence, positioning the insulation once inside (covered by plaster), once outside (covered by plaster), once at the middle (squeezed between two bricks of half the thickness compared to the other). Results showed that yearly transmission loads were unaffected by insulation location, whereas insulation location had a significant effect on the yearly averaged time lag and decrement factor, pointing out the wall with insulation at the middle

those with maximum temperature swings and the wall with insulation outside those with the smallest fluctuation.

In 2013, Kontoleon [23] carried out a more complex analysis compared to previous studies, determining the time lag and the decrement factor for walls, still made of the same thicknesses of insulating and capacitive material (concrete in this case, with variable density), but not limited to exploration of middle, outer and inner position of the insulation. The results showed how the concrete density and conductivity variations as well as the relative placement of concrete and insulation (in one or two layers within the wall assembly) affect the decrement factor and time lag, identifying the best wall assembly (among the 6 overall considered). In 2016, Kontoleon [24] continued the study by analysing the moisture storage effects on decrement factor and time lag of different walls.

In 2018, Leccese et al. [17] by using an analytical model based on heat transfer matrix, explored the effects of continuous variations in the positioning and thickness distribution of the insulation material on the dynamic thermal performance (decrement factor and time lag) of different constructive solutions (from a light-weight wall with a surface mass of 85 kg/m^2 to a massive wall with a surface mass of 294 kg/m^2).

In 2018, also Gori et al. [25], using a similar approach of [17], investigated if effective thermophysical properties can be determined for arbitrary multilayer walls, in order to represent them through equivalent homogeneous models, to be used in evaluations relating to the optimization decrement factor and time lag for opaque building envelopes. The obtained results indicated that, on the one hand, the equivalent thermal conductivity is determined simply by imposing the equivalence of the steady-state behaviour. On the other hand, the equivalent volumetric heat capacity (parameter that comes into play in dynamic conditions) is less immediate to determine and the authors propose two types of approximations to replace its exact value.

In 2022 Lu et al. [26] used the thermal quadrupole method to optimize (with reference to decrement factor and time lag) the location and distribution of the insulation layers of an external wall. In 2024, again Lu et al. [27] provided the analytical solutions of the wall's decrement factor and time lag using the auxiliary function method. The results the results obtained provided interesting insights for the passive thermal design of the building envelope, especially showing the influence of various parameter (i.e. dimensionless thickness, dynamic Biot number, thermal resistance, thermal diffusion, outdoor air temperature fluctuation period) on decrement factor and time lag of single layer wall.

As is evident, most studies have focused on providing solutions of the heat transfer equations and design criteria for optimizing the dynamic thermal behaviour of the external (envelope) walls, considering the decrement factor and time lag as intrinsic characteristics of the external walls. However, the passive thermal behaviour of a building is influenced also by the presence of internal elements (partition walls, slabs, furniture), for this reason a choice of the external wall assembly, made exclusively on the basis of the traditional decrement factor and time lag, seems to be a little simplistic [28].

In this paper the authors try to fill this research gap, providing a more complex calculation model, with which the dynamic thermal performance of the building envelope can be studied, also considering the presence of internal partitions (walls and floors) and furnishings. Furthermore, using the calculation model, detailed analysis of the influence of the internal elements and of the furnishings on the room thermal balance is reported. Then, the resistance-capacity distribution minimizing the decrement factor, in the external wall, is determined once the internal elements and the external wall's thermal resistance and capacity have been assigned. Finally, practical examples are shown. The results shown may be relevant for technicians dealing with the design of the building envelope, in order to understand the passive behaviour of the building more completely and to select the most appropriate technological solutions, in terms of wall assembly, in order to minimize the interventions of air conditioning systems.

3. Heat transfer model of the room and problem statement

The scheme representing the room being here examined is reported in Fig. 1. The external wall has area S. The sol–air temperature T_{ext} is assumed to be the outdoor air temperature. The interior of the room is assumed to be composed of M internal elements (partitions, floor and ceiling) the generic of which is assumed to have area S_m. Inside the room there is a heat source provided, for instance, with a heating/cooling plant. Let Q_S be the heat power, per surface unit of the external wall, supplied by the above-stated heat source. Heat transfer is assumed to be one dimensional; any effect due to the thermal bridges will be disregarded.

Under conditions of periodic thermal regime, the external thermal field T_{ext} and the internal one T_{int}, the heat power Q_S, the heat fluxes q_{ext} and q_{int}, respectively on the outer and inner surface of the external wall, are to be considered periodic functions of the time τ developable in Fourier series; farther on by T_{ext}, T_{int}, Q_S, q_{ext} and q_{int} the generic harmonic components of angular frequency ω (with period $P=2\pi/\omega$) of the above-mentioned series will be meant.

The linear relation, subsisting between the temperature T_{int}, the heat flux q_{int} and the analogous quantities T_{ext} and q_{ext}, can be determined using the heat transfer matrix method according to Eq. (1):

$$\begin{pmatrix} T_{int} \\ q_{int} \end{pmatrix} = \begin{pmatrix} E & F \\ G & H \end{pmatrix} \times \begin{pmatrix} T_{ext} \\ q_{ext} \end{pmatrix} \tag{1}$$

The heat transfer matrix method, also referenced as thermal quadrupole method [29–31], is well known in the scientific and technical literature [32,19] and widely used for describing heat conduction in one—dimensional structures [33,34]. The method was the subject of numerous validations, which have proven its effectiveness for this type of analysis [35–37]. By reference, essential details of the method are reported in Appendix 1. The matrix in Eq. (1) has unitary determinant ($EH-FG=1$) and will have to be calculated as ordered product of the transmission matrices of the single layers making up the wall; the first and the last of these layers will be purely resistive ones, representing, respectively, the wall inner surface thermal resistance r_{int} and the wall outer surface thermal resistance $r_{ext.}$. Farther on, the external wall overall thermal resistance and capacity will be indicated, respectively, by r and c.

For the m-th internal element the following equation, analogous to the Eq. (1), is still valid:

$$\begin{pmatrix} T'_{int} \\ q'_{m} \end{pmatrix} = \begin{pmatrix} e_m & f_m \\ g_m & h_m \end{pmatrix} \times \begin{pmatrix} T_{int} \\ q_{m} \end{pmatrix} \tag{2}$$

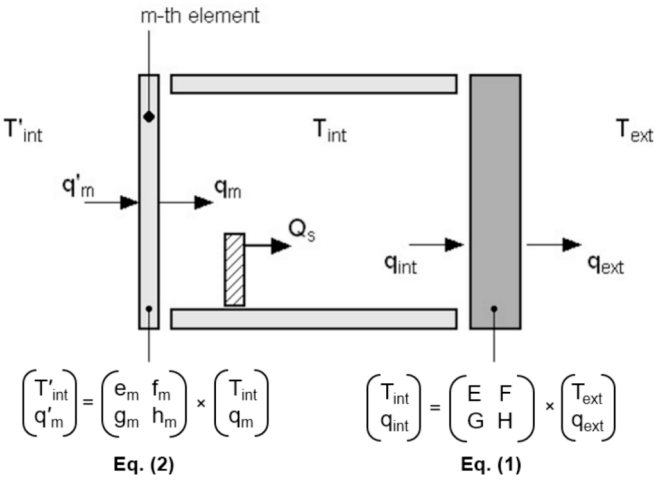

Fig. 1. Scheme of the examined room.

having marked by the apex the temperature and flux relating to the adjacent room. In the Eq. (2) the matrix has unitary determinant and will have to be calculated as ordered product of the transmission matrices of the single layers making up the structure being here discussed; the outer layers will be purely resistive ones, representing the opportune wall inner and outer surface thermal resistances.

For the room, if the effects due to the air change are disregarded, with reference to the angular frequency ω and period P and with regard to the surface unit of the external wall, the following balance equation subsists [15]:

$$q_{int} + j\omega U T_{int} = Q_{int} + Q_S \tag{3}$$

where Q_{int} is the total flux concerning the internal elements, while the air lying in the room is schematized with a pure thermal capacity U, per surface unit of the external wall. From the Eq. (1) it follows that:

$$q_{int} = \frac{H \bullet T_{int} - T_{ext}}{F} \tag{4}$$

From the Eqs. (2), if the temperature in the adjacent rooms is supposed to oscillate, as it generally happens, with the same amplitude and phase as that of the examined room, $T'_{int} = T_{int}$, the following is obtained:

$$q_m = -\left(\frac{e_m - 1}{f_m}\right)\cdot T_{int} = -\lambda_m \bullet T_{int}$$

having introduced the admittance λ_m of the m-th internal element:

$$\lambda_m = \frac{e_m - 1}{f_m} \tag{5}$$

The quantity $\omega I_m(1/\lambda_m)$, product of the angular frequency ω by the imaginary part of $1/\lambda_m$, can be meant as the inverse of the thermal capacity per surface unit of the m-th internal element with regard to the face turned towards the examined room [19].

In many cases, the internal elements, with the exception of roof and ceiling, are symmetrical ($e_m = h_m$). The surface passing through the centre plane of the m-th partition can be schematized as adiabatic with the temperature T_{0m}; consequently, just half of the partition turned towards the room turns out to be concerned with the room heat problem. In these conditions, instead of the Eq. (2), the following can be written:

$$\begin{pmatrix} T_{0m} \\ 0 \end{pmatrix} = \begin{pmatrix} \bar{e}_m & \bar{f}_m \\ \bar{g}_m & \bar{h}_m \end{pmatrix} \times \begin{pmatrix} T_{int} \\ q_m \end{pmatrix} \tag{6}$$

In the Eq. (6) the matrix elements refer to half of the examined partition. From the Eq. (6) it follows:

$$\bar{q}_m = -\frac{\bar{g}_m}{\bar{h}_m}\cdot T_{int} = -\lambda_m \bullet T_{int}$$

It can be concluded that the admittance λ_m of a symmetric partition can be easily calculated as:

$$\lambda_m = \frac{\bar{g}_m}{\bar{h}_m} \tag{7}$$

In any case, the term Q_{int} of the Eq. (3) can be calculated by the following relation:

$$Q_{int} = \frac{1}{S}\sum_{m=1}^{M}(S_m q_m) = -T_{int} \bullet \sum_{m=1}^{M}(\lambda_m \alpha_m) \tag{8}$$

with $\alpha_m = S_m/S$ the "weight" of the m-th internal element.

In absence of heating/cooling plant, wishing to study the room purely passive behaviour, from the Eq. (3) with Q_S=0, the ratio ζ between the indoor air temperature and the outdoor one can be calculated; this ratio turns out to be, for the Eqs. (4) and (8), the following:

$$\zeta = \frac{T_{int}}{T_{ext}} = \frac{1}{H + F\Lambda} \tag{9}$$

having introduced the quantity Λ, depending on the structure and geometry of the room, defined by:

$$\Lambda = j\omega U + \sum_{m=1}^{M}(\lambda_m \alpha_m) \tag{10}$$

This quantity can be meant as the overall admittance of the internal elements, since in an electric analogy it represents the inverse of the impedance of the grid formed by a parallel to the branches of which the indoor air and the internal elements contribute. Obviously, the admittance relating to the air jωU (pure imaginary term) is just a corrective term; to a first approximation, we could think of lumping together in this term the capacitive effects of the objects (furniture, furnishings, etc.) lying in the room. For a more careful evaluation of the influence of the furnishings see the Appendix 2. The quantity $|\Lambda|/\omega$ is sometimes indicated as thermal capacity of the internal elements.

The following can be posed:

$$\zeta = \sigma \cdot e^{-j\omega\tau_R}$$

having introduced the decrement factor σ of the amplitude of the outdoor air temperature variation imposed on the outside and the time lag τ_R defined by:

$$\sigma = |\zeta| \quad \tau_R = \frac{1}{\omega}\cdot\arctan\left[\frac{Im(\zeta)}{Re(\zeta)}\right] \tag{11}$$

Obviously, σ and τ_R depend on the following factors: the external wall thermal properties due to the matrix elements H and F; the internal elements' thermal properties due to Λ, and the period P of the outdoor temperature variation. The smaller σ is, the higher the room dynamic thermal insulation will be, i.e. the less the indoor conditions will depend on the outdoor ones.

As far as the time lag τ_R is concerned, it can be observed that the thermal loads being involved are essentially due to the solar radiation transferred through windows, to the energy required for the thermal treatment of the exchanged air, and, finally, to the heat transfer through the building envelope opaque wall. The first two thermal loads are substantially in phase with the outdoor temperature variation; an outstanding reduction in the maximum thermal load could then occur by designing the walls so as to delay favourably, as to the outdoor temperature variations, the thermal load due to the heat transfer through the building external walls. The periods P of practical interest are the following: P=1h, which corresponds to very short time variations, such as the ones relating to temperature control systems; P=24 h, which corresponds to daily weather and temperature variations; a week corresponding to longer-term averaging of the building, and a year, useful for the treatment of the heat transfer through the ground.

4. Resistance-capacity distribution optimization

This problem consists in minimizing the decrement factor σ, for given values of the overall thermal resistance (R) and capacity (C), for the realization of both external walls and internal elements. This problem is very simple and can be easily solved analytically. Under steady conditions, from an energy point of view, the convenience of distributing the overall resistance as much as possible within the external wall is evident. Under these conditions, the internal elements can be schematized as a pure thermal capacity c_{int}.

For the external wall a lumped-capacitance scheme is considered subdividing the wall into n capacitive layers, each of them with capacity c_s (s = 1..n), and into n resistive layers, each of them with resistance r_s; the capacity of the innermost layer of the external wall is indicated by $\hat{c}_n$. The room can be, then, represented by the following scheme [17]:

$[c_{int}]$ [int] $[\hat{c}_n]$ $[r_n]$……..$[r_2]$ $[c_1]$ $[r_1]$ [ext]

The indoor air temperature and the internal wall temperature are identical in the adopted schematization. Writing $c_n = \hat{c}_n + c_{int}$, the previous scheme (named Γ_n because it is composed of n resistive layers and n capacitive layers) can be posed in the following form:

[int] $[c_n]$ $[r_n]$……..$[r_2]$ $[c_1]$ $[r_1]$ [ext]

It is easy to verify that, under such conditions, we simply have:

$$\sigma = \frac{1}{|H|}$$

where H is the second-raw and second-column of the transmission matrix of the wall represented with the scheme Γ_n.

The optimal sequence of resistances and capacities in the scheme Γ_n will be that maximizing the module of H by the following conditions: $\Sigma r_s = R$ and $\Sigma c_s = C$. Farther on, the square of the module of H, relating to the scheme Γ_n will be indicated by ϕ_n. Under these hypothesis, the choice of the wall optimal scheme is completely determined by a single parameter $\mu = \omega RC$. According to the value of μ, optimal schemes with very different characteristics can be obtained. The analysis can be developed beginning from the lowest values of n, looking for the conditions being able to maximize the quantity ϕ_n.

For $n = 1$ the scheme Γ_1 (composed of one resistive and one capacitive layers) is unique and turns out to be of the following type:

[int] [C] [R] [ext]

characterized by the transmission matrix

$$\begin{pmatrix} 1 & 0 \\ j\omega C & 1 \end{pmatrix} \times \begin{pmatrix} 1 & R \\ 0 & 1 \end{pmatrix}$$

It follows that:

$$H = 1 + j\mu \quad \phi_1 = 1 + \mu^2 \quad \sigma = \frac{1}{\sqrt{\phi_1}} = \frac{1}{\sqrt{1+\mu^2}}$$

and the decrement factor σ decreases rapidly with μ.

It is easy to guess that the scheme Γ_1, in which all the available thermal resistance is disposed on the external wall outer face, turns out to be the optimal one just for low values of μ. This is confirmed by the analysis of the case with $n = 2$ (scheme Γ_2, wall composed of two resistive and two capacitive layers).

In the case $n = 2$ we have the following scheme Γ_2:

[int] $[c_2]$ $[r_2]$ $[c_1]$ $[r_1]$ [ext]

with $r_1 + r_2 = R$; $c_1 + c_2 = C$. After developing calculations, the following is obtained:

$$H = 1 - \mu^2 \frac{c_1 c_2 r_1 r_2}{C^2 R^2} + j\mu \frac{c_1 r_1 + c_2 r_1 + c_2 r_2}{CR}$$

If a maximum exists for the module of H, it obviously has to occur for $c_2/C = r_1/R$; indicating this common value by z ($z = c_2/C = r_1/R$), it will be enough to look for the maximum of

$$\phi_2 = 1 + \mu^2 z^2 (2 - z^2) + \mu^4 z^4 (1 - z)^4$$

For low values of μ, this function is increasing with z ($0 < z < 1$); for μ lower than 11 a relative maximum arises whose value is lower than the absolute maximum localized in $z = 1$; for $\mu > 11$ the value of the interior maximum exceeds the value in $z = 1$ (i.e. it becomes an absolute maximum). More precisely, for $\mu = 11$ the maximum value of the module of H is reached for $z = 0.618$.

In other words, 11 turns out to be the value of μ for which the scheme with $n = 2$ becomes more convenient than that with $n = 1$. For such a value, the resistances and capacities of the optimal schemes are the following $r_1/R = c_2/C = z \approx 0.618$, $r_2/R = c_1/C = 1 - z \approx 0.382$. The scheme Γ_2 remains optimal as long as the parameter μ does not exceed a new threshold value, which can be analysed studying analogously the scheme Γ_3 (wall composed of three resistive and three capacitive layers) and so on. The calculations obviously become increasingly heavy as n increases, and for $n > 2$ it results to be easier to proceed numerically. The obtained results are summarized in Table 1. The values of the resistance (r_s/R) and capacity (c_s/C) ratios of the various layers, necessary for the realization of the corresponding optimal schemes, versus μ are represented in Fig. 2. The trend of the so optimized decrement factor σ versus μ is shown in Fig. 3.

A simple approximated solution of the problem consists in assuming as nearly-optimal schemes, those with the resistance-capacity ratios equal for all the layers

$$\frac{r_s}{R} = \frac{c_s}{C} = \frac{1}{n}$$

It is easy to calculate for the schemes, with n from1 to 3, the expressions for the element H of the transmission matrix. The calculation results are summarized in Table 2, where $p_n = \mu/n^2$.

The first of them is clearly exact, the other ones provide values of the optimal decrement factor σ with the approximation of the 3 % for $\mu < 60$; this shows that the subdivision into equal parts of the available resistance and capacity represents, in each of the above-indicated intervals of μ, a reasonable practical realization of the optimal conditions.

The influence of the thermal resistances relating to the internal elements and, in particular, of the surface thermal resistance, localized between such elements and the indoor air, can result to be remarkable; the presence of this surface thermal resistance determines, in some cases, an increase in the decrement factor σ, while, in other cases, it determines a small reduction of σ.

5. Analysis of the room internal elements influence

In the previous section room internal elements have been schematized as a pure thermal capacity. Such a schematization is drastic. In fact, if several insulating materials (e.g. polyurethane, polystyrene, etc…) are assimilable, with optimal approximation, to pure thermal resistances, currently there are very few materials (e.g. phase-change materials) assimilable to pure thermal capacities. Besides, the inner and outer surface thermal resistances relating to the internal elements are not negligible and can have a remarkable influence. In this section, the influence of the internal elements on the periodic heat transfer is analysed, considering the complex quantity Λ, and some examples are shown to discuss this influence.

The influence of the internal elements on the quantity Λ, according to its definition through Eq. (10) is exerted by the complex admittance λ. For determining λ, a partition wall composed of a homogeneous layer with thickness x was considered. The partition wall has equal inner and outer surface thermal resistances $r_{int} = 0.13\ m^2 \bullet K \bullet W^{-1}$ (symmetric partition) [38]. In such conditions, the transmission matrix results to be

Table 1
Calculation results: ranges of μ for which each wall scheme is convenient.

Scheme ID	Number of layers	Layers features	Range of μ for which the scheme is convenient
Γ1	2	one resistive (disposed on the outside) and one capacitive layers	$0 < \mu \leq 11$
Γ2	4	two resistive and two capacitive layers (alternated)	$11 < \mu \leq 31$
Γ3	6	three resistive and three capacitive layers (alternated)	$31 < \mu \leq 60$

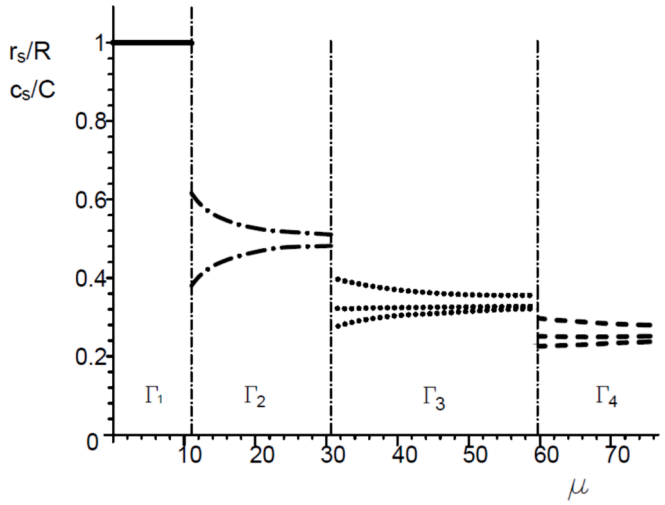

Fig. 2. Variation of r_s/R and of c_s/C with μ. Zone Γ_1: the segment shows $r_1/R=c_1/C=1$. Zone Γ_2: the upper curve shows $r_1/R=c_2/C$, the lower curve shows $r_2/R=c_1/C$. Zone Γ_3: from the top to the down the curves show $r_1/R=c_3/C$; $r_3/R=c_1/C$; $r_2/R=c_2/C$. Zone Γ_4: from the top to the bottom the curves show $r_1/R=c_4/C$; $r_4/R=c_1/C$; $r_2/R=c_3/C$; $r_3/R=c_2/C$.

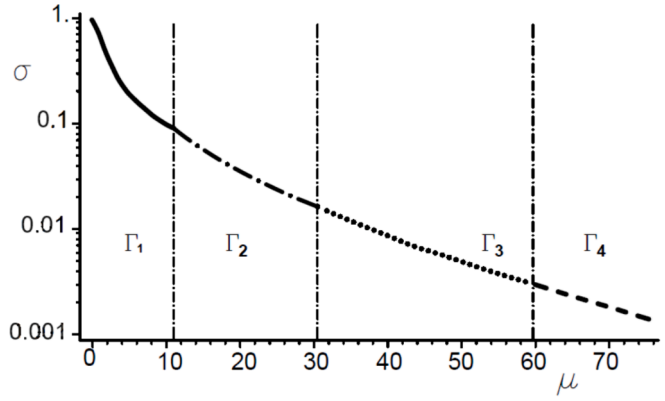

Fig. 3. Variation of optimized decrement factor σ with μ.

Table 2
Expressions for the element H of the transmission matrix, in the case of $r_s/R=c_s/C=1/n$ and n ranging from 1 to 3.

n	p_n	H_n
1	μ	$1 + j\ p_n$
2	μ/4	$1 + j\ p_n\ (3\text{-}p_n)$
3	μ/9	$1 + j\ p_n\ (6\text{-}5p_n\text{-}p_n^2)$

the following:

$$\left(\bar{e}\,\bar{f}\bar{g}\bar{h}\right) \times \begin{pmatrix} 1 & r_{int} \\ 0 & 1 \end{pmatrix} = \left(\bar{e}\,\bar{e}r_{int} + \bar{f}\bar{g}\bar{g}r_{int} + \bar{h}\right)$$

The admittance λ can be calculated according to Eq. (7), resulting in

$$\lambda = \frac{\lambda_0}{1 + r_{int}\lambda_0} \tag{12}$$

with $\lambda_0 = \sqrt{j}\,\lambda_\infty \tanh\left(\sqrt{2j}\ \frac{x}{\nu}\right)$.

By way of example, some commonly used materials for the creation of building partitions were considered. The thermophysical characteristics of the considered materials are summarized in Table 3, where: ρ ($kg\bullet m^{-3}$) is density, C_p ($kJ\bullet kg^{-1}\bullet K^{-1}$) the specific heat at constant pressure, k ($W\bullet m^{-1}\bullet K^{-1}$) the thermal conductivity, $\xi = \rho C_p k$ ($J\bullet W\bullet m^{-4}\bullet K^{-2}$) the thermal effusivity and $\beta = k/(\rho C_p)$ ($m^2\bullet s^{-1}$) the thermal diffusivity. In Table 3 the penetration depth values of a temperature variation within a semi-infinite solid $\nu = \sqrt{2\beta/\omega}$ and the conductance $\lambda_\infty = \sqrt{\omega\xi}$ (both calculated for a 24 h period) are also reported.

In the Fig. 4 and Fig. 5, the trends of |λ| and θ versus the thickness x are respectively reported. The trends, for the different materials that build-up the partition wall, were obtained from Eq. (12) considering an oscillation period P=24 h. The trend for the material brick-2 (see Tab. 3) is similar to those of the other bricks and placed between the trends brick-1 and brick-3. The same happens for the material concrete-2 (see Tab. 3) with respect to the other concretes. As can be seen from the trends, for low values (approximately lower than 0.1 m) of x, |λ| tends to increase (and θ to decrease) with the increase of x, leading to an increase of Λ, keeping constant admittance relating to the air and constant geometry of the room (see Eq. (10)). For medium values of x (generally

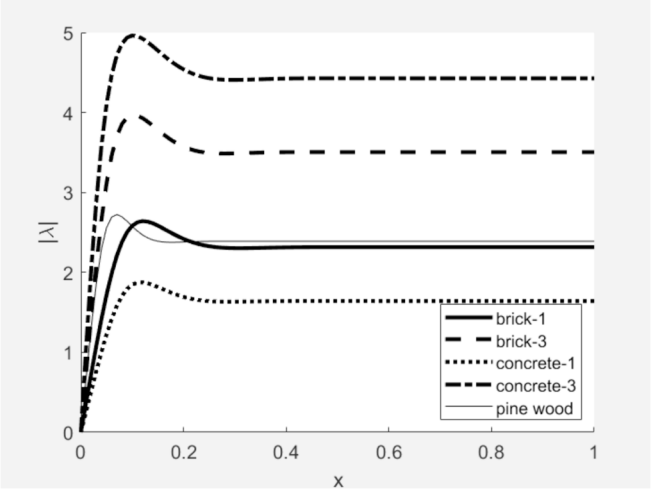

Fig. 4. Trends of |λ| ($W\bullet m^{-2}\bullet K^{-2}$) versus x (m), for P=24 h and with r_{int} = 0.13 $m^2\bullet K\bullet W^{-1}$.

Table 3
Thermal properties of the considered materials.

Material	ρ (kg/m^3)	C_p (kJ/kgK)	k (W/mK)	ξ·10^{-5} (J^2/sm^4K^2)	β 10^7 (m^2/s)	ν (m)	λ_∞ (W/m^2K)
Brick-1	600	0.84	0.25	1.26	4.96	0.117	3.03
Brick-2	1000	0.84	0.35	2.94	4.17	0.107	4.62
Brick-3	1200	0.84	0.43	4.33	4.27	0.108	5.61
Concrete-1 (cellular)	400	0.88	0.15	0.528	4.26	0.108	1.96
Concrete-2 (cellular)	600	0.88	0.20	1.06	3.79	0.102	2.77
Concrete-3 (lightweight)	1600	0.88	0.70	9.86	4.97	0.117	8.47
Pine wood	550	1.66	0.15	1.37	1.64	0.067	3.16

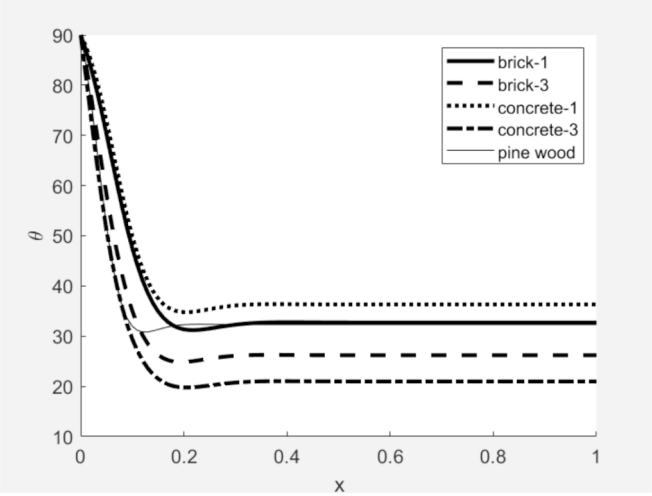

Fig. 5. Trends of θ (deg) versus x (m), for P=24 h and with r_{int} = 0.13 m^2•K•W^{-1}.

between 0.1 m and 0.3 m), |λ| reaches the maximum value and then decreases as x increases. The maximum of |λ |, even if not very significant from a practical point of view, involve a minimum for the room decrement factor, and point out resonance effects due to the internal elements [39]. For large values of x (generally higher than 0.3 m, rather large compared to the typical thicknesses of partition walls realized in contemporary building), |λ| reaches a saturation value independent of x, but dependent on the material. For the different materials, the saturation values can be predicted considering that, for x≫ν, |λ| and θ are given by:

$$|\lambda| = \frac{\lambda_\infty}{\sqrt{1+\sqrt{2}r_{int}\lambda_\infty + (r_{int}\lambda_\infty)^2}} \quad \theta = \arctan\left(\frac{1}{1+\sqrt{2}\,r_{int}\lambda_\infty}\right) \tag{13}$$

The saturation values, calculated using Eqs. (13) are shown in Table 4, for all the considered materials. For completeness, in Figs. 6 and 7 the saturation values are shown, considering the possible values of the surface thermal resistance on the face of the partition looking onto the considered room (i.e. 0.13 m^2•K•W^{-1} for horizontal heat flux, 0.10 m^2•K•W^{-1} for upward heat flux, 0.17 m^2•K•W^{-1} for downward heat flux, indicated by the technical standards [38]).

In some cases, for essentially aesthetical reasons, the partitions (horizontal and vertical) are covered with layers made of particular materials: plaster, wood, carpeting etc. For the investigation of the effects caused by these coverings, as examples two Brick-3 walls were considered, the first being 25 cm in thickness, the second 12 cm. In both cases the coverings are assumed as symmetrically applied on the two faces of the wall, and calculations were developed for P=24 h, with equal surface thermal resistances r_{int} = 0.13 m^2•K•W^{-1}. The following three types of covering material were considered: a material with essentially capacitive properties, such as the lime-mortar plaster with thermal effusivity higher than that of the Brick-3; a material with essentially resistive properties, such as the polyurethane with thermal effusivity sensibly lower than that of the Brick-3, and, finally, a material with resistive and capacitive thermal properties, such as fir-wood, with thermal effusivity lower than that of the Brick-3. The thermal properties of the covering materials are shown in Table 5.

Table 4
|λ| and θ saturation values for different materials, for P=24 h and with r_{int} = 0.13 m^2•K•W^{-1}.

Material	|λ| (Wm^2K)	θ (deg)
Brick-1	2.15	37.83
Brick-2	2.80	29.50
Brick-3	3.11	26.05
Concrete-1 (cellular)	1.56	47.47
Concrete-2 (cellular)	1.86	42.24
Concrete-3 (lightweight)	3.79	19.16
Pine wood	2.21	36.95

In Fig. 8, the trends of |λ| versus the thickness y of the additional layer for the two considered walls is reported. In the figure, the bold curves are referred to the 25 cm thick wall, and the thin curves are referred to the 12 cm thick wall. The curves relating to the addition of plaster, fir-wood and polyurethane were marked by the following letters: PL, FW, and PO respectively.

From the figure it is clear that the application of a plaster layer always involves an increase in |λ| with consequent increase in |Λ| and decrease in σ (see Eqs. (9) and (10)). On the contrary, the application of a covering layer with an effusivity lower than that of the brick (polyurethane and also fire-wood) always involves a decrease in |λ |, with consequent decrease in |Λ| and increase in σ. The trends of the phase θ versus y is more complex and the curves referred to the addition of plaster, wood and polyurethane may show some minimums. In any case, the addition of a material with thicknesses of practical interest (y < 5 cm) always leads to a slight decrease in θ. Obviously, according to the Eq. (10), the admittance λ of the internal elements has to be weighed by the corresponding geometrical factor α, which becomes very important for the determination of the final value of Λ. Generally, for the most common elements and for P=24 h, the values |Λ| are in the range 5 ÷ 50 $Wm^{-2}K$, and they are significantly dependent on the parameters discussed in this section.

6. Optimization of the external wall considering the room internal elements influence

This problem consists in determining the resistance-capacity distribution within the external wall minimizing the decrement factor σ, having assigned: the room internal elements (and then Λ), the external wall overall thermal resistance r and overall thermal capacity c.

According to Eqs. (9) and (11), the decrement factor σ can be calculated as

$$\sigma = \frac{1}{|H + F\Lambda|} \tag{14}$$

Introducing $\widetilde{F} = F/r$ and D=r | Λ |, Eq. (14) can be rewritten as:

$$\sigma = \frac{1}{\left|H + \widetilde{F}D\right|} \tag{15}$$

From equation (15) and the definitions of H and F (indicated in the technical standards [19] and also deducible from Appendix 1), it is possible to demonstrate that optimal external wall stratigraphy turns out to depend only on the three dimensionless parameters D, γ (γ = ωrc) and φ (phase of Λ). The optimization methodology can be discussed by treating the following three cases separately.

6.1. Optimization for heavy internal elements

In the case of internal elements with |F•Λ|≫|H| (this condition is generally satisfied when elements are heavy and with remarkable thermal capacity), according to the Eq. (14), the following can be considered:

$$\sigma \approx \frac{1}{|F\Lambda|}$$

Considering a fixed value of | Λ|, the optimal external walls are those maximizing |F |.

This problem was already addressed in previous studies [15,40], in

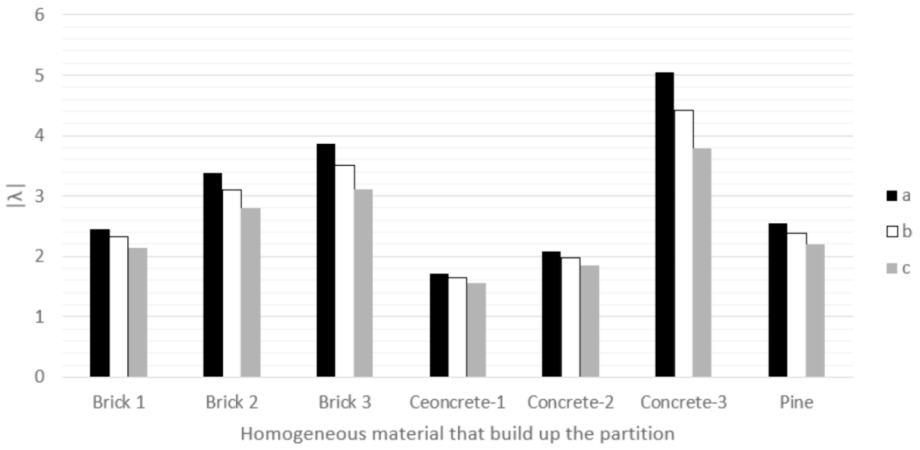

Fig. 6. Values of $|\lambda|$ ($W \bullet m^{-2} \bullet K^{-2}$) obtained from Eq. (13) for different materials: a) $r_{int} = 0.10\ m^2 \bullet K \bullet W_{,}^{-1}$ b) $r_{int} = 0.13\ m^2 \bullet K \bullet W_{,}^{-1}$ c) $r_{int} = 0.17\ m^2 \bullet K \bullet W^{-1}$.

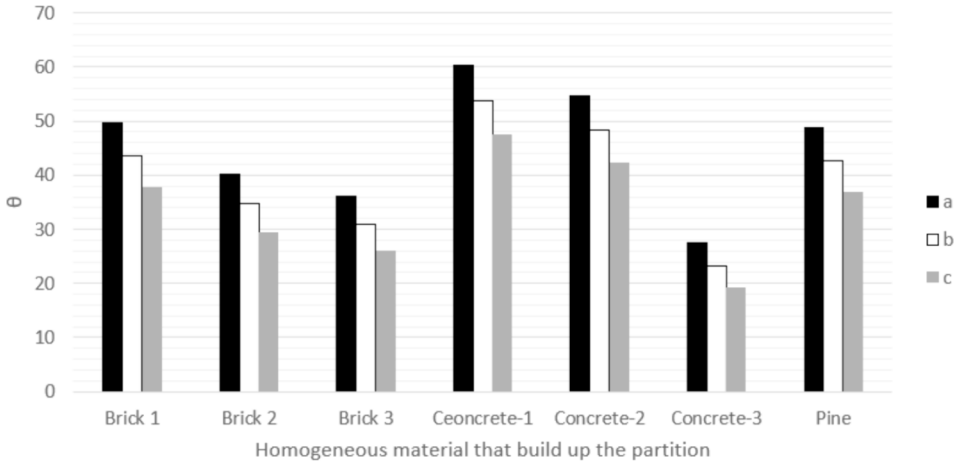

Fig. 7. Values of θ (deg) obtained from Eq. (13) for different materials: a) $r_{int} = 0.10\ m^2 \bullet K \bullet W_{,}^{-1}$ b) $r_{int} = 0.13\ m^2 \bullet K \bullet W_{,}^{-1}$ c) $r_{int} = 0.17\ m^2 \bullet K \bullet W^{-1}$.

Table 5
Thermal properties of the considered covering materials.

Material	ρ (kg/m³)	C_p (kJ/kgK)	k (W/mK)	$\xi \cdot 10^{-5}$ (J^2/sm^4K^2)	β 10^7 (m^2/s)	ν (m)	λ_∞ (W/m^2K)
Lime-mortar plaster	1800	0.91	0.8	13.1	4.88	0.116	9.762
Polyurethane	35	1.6	0.035	0.0196	6.25	0.131	0.378
Fir-wood	450	1.38	0.12	0.745	1.93	0.073	2.328

in which it was highlighted that the optimized resistance-capacity distributions within the external wall are representable by the following scheme (named T_n and composed of n capacitive layers and n + 1 resistive layers):

[int] [r_{n+1}] [c_n] [r_n]……..[r_2] [c_1] [r_1] [ext]

The wall has been subdivided into n purely capacitive layers, each of them with thermal capacity cs (s = 1..n), and into n + 1 purely resistive layers, each of them with thermal resistance rs (s = 1..n + 1); the different layers are disposed in sequence, alternating a resistive layer and a capacitive one.

The transmission matrix of a wall representable with the scheme (T_n) is given by the following product:

$$\begin{pmatrix} 1 & r_{n+1} \\ 0 & 1 \end{pmatrix} \times \begin{pmatrix} 1 & 0 \\ j\omega c_n & 1 \end{pmatrix} \times \begin{pmatrix} 1 & r_n \\ 0 & 1 \end{pmatrix} \times \ldots \times \begin{pmatrix} 1 & r_2 \\ 0 & 1 \end{pmatrix} \times \begin{pmatrix} 1 & 0 \\ j\omega c_1 & 1 \end{pmatrix} \times \begin{pmatrix} 1 & r_1 \\ 0 & 1 \end{pmatrix}$$

Obviously, for large n the scheme (T_n) can approximate well any distributed-parameter real wall.

Introducing the parameter γ, such optimization results can be briefly resumed as follows.

For γ < 18, the symmetrical scheme T1 (with n = 1) turns out to be optimal, that is, a three-layer wall with the capacitive layer (c) disposed between two equal resistive ones (r/2):

[int] [r/2] [c] [r/2] [ext]

For 18 < γ < 42 a scheme with n = 2 results to be optimal, that is to say, a five-layer wall with three resistive and two capacitive ones:

[int] [r3] [c2] [r2] [c1] [r1] [ext]

For 42 < γ < 76 a scheme with n = 3 (seven-layer wall) turns out to be optimal. The optimal resistance and capacity values to be assigned to the different layers are analysed in [40]; a good approximation is obtained assuming the same values for all the resistances and capacities of the different layers [40].

For γ→∞ the optimal wall tends to a homogeneous wall with uniformly distributed resistive and capacitive parameters.

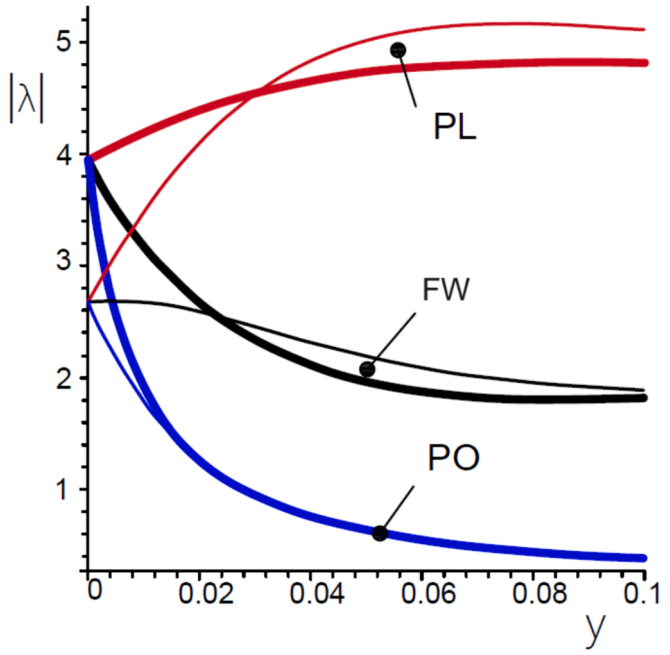

Fig. 8. Brick-3 wall with P=24 h. Variation of |λ| with y: wall 25 cm in thickness, bold curves; wall 12 cm in thickness, thin curves. The curves relating to the addition of plaster, wood and polyurethane were marked by the following letters: PL, FW, and PO respectively.

In South Europe the walls composing the building envelope show very often values of $\gamma < 18$; just in the case of particularly massive walls with remarkable thicknesses of the resistive layer it can results $\gamma > 18$. However, in these cases, almost in all the situations of interest, it results $\gamma < 42$.

6.2. Optimization for light internal elements

In the case of internal elements with $|F\bullet\Lambda| \ll |H|$ (this condition is generally satisfied if elements are light and with small thermal capacity) the following can be written according to the Eq. (14),

$$\sigma \cong \frac{1}{|H|}$$

The optimal external walls are those maximizing |F |. This problem was already addressed in previous Section 4 and coincide with those with the scheme Γ_n (composed of n capacitive layers and n resistive layers), on condition that γ will be replaced with μ (see Section 4 for full details).

6.3. Optimization for generic internal elements

When $|F\bullet\Lambda|$and |H| are comparable, the complex numbers, which are at the denominator in the definition of σ (see Eqs. (14) and (15)), add and the phase of Λ (φ) also plays a relevant role. In this case, the optimal solution could be either a T_n scheme or an Γ_n scheme, according to the value of γ. Hence, the optimization problem consists in determining, for given D and φ, the resistance-capacity distribution within the external wall capable to minimize σ, in function of γ, according to the schemes T_n and Γ_n.

The method adopted to solve this problem is the same as that used in Section 4; in this case calculations become very heavy even for small values of n. The problem was numerically solved for an outdoor air temperature variation with P=24 h. Some of the obtained results are summarized in Figs. 9 and 10, in order to show the considerations that should be conducted for the purpose of determining the optimal resistance-capacity distribution within the external wall.

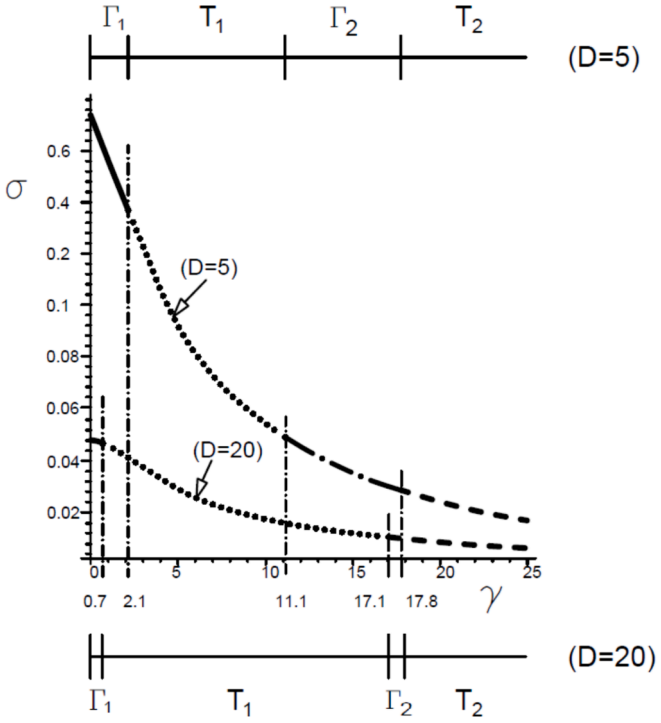

Fig. 9. Optimal schemes and variation of σ with γ for φ = π/4 and for two values of D (D=5 and D=20).

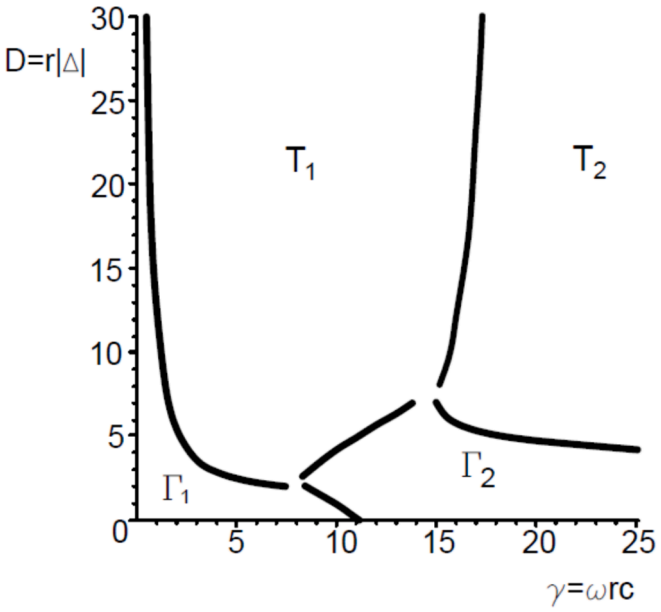

Fig. 10. The case of φ = π/4. The zones Γ_1, T_1, Γ_2, T_2 are delimited by limit curves showing the change from an optimal scheme to another.

In Fig. 9, the trends of σ with γ for two values of D (D=5, D=20) and for φ = π/4 are reported. For D=5 (solid-line curve) the optimal external walls are: Γ_1 for $0 < \gamma < 2.1$; T_1 for $2.1 < \gamma < 11.1$; Γ_2 for $11.1 < \gamma < 17.8$; T_2 for $\gamma > 17.8$. For D=20 (dashed curve) the optimal external walls are: Γ_1 for $0 < \gamma < 0.7$; T_1 for $0.7 < \gamma < 17.1$; T_2 for $\gamma > 17.1$.

In Fig. 10, an analysis of the way in which the resistance-capacity distribution varies as D and γ vary, is shown for φ = π/4. In the figure, the zones characterized by different schemes are pointed out; such zones are delimited by limit curves showing the change from an optimal scheme to another. For low values of D, the optimal scheme Γ_n is

convenient; in particular, for $\gamma < 11$ the scheme Γ_1 turns out to be optimal, while, for $\gamma > 11$ the scheme Γ_2 is to be preferred, in accordance with Section 4. For high values of D (D>≈20), the scheme T_n is convenient; in particular for γ<≈18, the scheme T1 turns out to be optimal, while, for γ>≈18, the scheme T2 is to be preferred, in accordance with Section 6.1. For mean values of D, for instance, D=5, it turns out to be clear that, as γ increases, the external wall optimal scheme varies as follows: for $\gamma < 2.1$ it is of the type Γ_1, for $2.1 < \gamma < 11.1$ it is T_1, for $11.1 < \gamma < 17.8$ it is Γ_2 and, for $\gamma > 17.8$, it is T_2. For D higher than 10, the scheme Γ_2 is never optimal, and a direct change occurs from T_1 to T_2 ($\Gamma 1$ is optimal only for very low and of little practical interest values of γ).

Note that the results shown in the figure refer to the input data used by the authors, but the approach followed has general validity and can be repeated for various φ. An analogous analysis was made for example for values of φ differing from π/4. It is clear that the most remarkable differences occur for the central part of the Fig. 10 (mean values of D). By way of example, for D=5, the transition from the optimal scheme Γ_1 to the T_1 occurs at $\gamma = 0.9$ for $\varphi = \pi/8$, at $\gamma = 2.1$ for $\varphi = \pi/4$, and at $\gamma = 4.1$ for $\varphi = 3\pi/8$. Analogously, the transition from the scheme T1 to the Γ_2 occurs at $\gamma = 5.9$ for $\varphi = \pi/8$, at $\gamma = 11.1$ for $\varphi = \pi/4$, and at $\gamma = 14.2$ for $\varphi = 3\pi/8$. The values of σ calculated under optimal conditions for such phase values differ from each other by few percentage units (less than 5 %). Fig. 9 (and analogous graphs that can be made with different φ values) can be considered as a selection abacus, useful for identifying the optimal scheme. It can constitute an effective support tool for designers in the early design stage when the technical solutions to maximize the thermal resilience of the building are selected.

7. Limitations and future developments

The present study is a contribution to the ongoing discussion, in the scientific community, about the optimization of the opaque envelope to enhance thermal resilience of the buildings. In accordance with the complexity of the analytical treatment of the problems faced, this study presents the following limitations.

The oscillations of external environmental conditions (in particular sol–air temperature) of the present study are considered purely sinusoidal with a period of 24 h. The results shown and described in this paper refer exclusively to these conditions. Actually, the oscillations of external environmental conditions are, as is known, different from pure sinusoids. However, the validity of the method is not compromised, because results similar to those shown can be obtained, with the use of the described method, for generic fluctuations of external conditions, breaking down the generic fluctuation into a sum of sinusoidal fluctuations using harmonic analysis.

The materials used for the analyses in the present study (see in particular Table 3 and Table 5), obviously, do not cover all the commercially available solutions. They should be considered as significant examples. Nowadays, designers have a vast range of products at disposal with which to compose their own technical solutions. However, the proposed optimization methodology remains valid regardless of the material used.

To date, no experimental validations of the described results are available. This element represents a possible future development of the study. However, as indicated in the text (see Section 3), the heat transfer matrix method on which this study is based has been validated by numerous studies and its effectiveness widely proven by the scientific literature.

8. Conclusions

In the present paper, the distribution of given thermal resistance and capacity between the external wall and the internal elements was studied within a lumped-capacitance schematization and in absence of heating/cooling plants. More precisely, the distribution minimizing the decrement factor σ and then optimizing the building purely passive behaviour was sought. The obtained result indicates the optimal situation to be that in which the internal elements results to be completely capacitive, while the external wall should be realized alternating resistive layers with capacitive ones by a sequence depending on a single parameter μ (product of angular frequency of external temperature oscillations, overall thermal resistance and overall thermal capacity of both external wall and internal elements). Such a solution clearly seems to be hardly realizable, even in an approximated way, in the building practice.

For a higher closeness to practical applications, the internal elements (partition wall and slabs) of the room were schematized with a distributed-parameter structure provided with complex admittance Λ. After analysing the influence of the internal elements on the room admittance, the optimal stratigraphy of the external wall (having thermal resistance r and thermal capacity c assigned) was determined, in order to minimize the decrement factor σ. The results obtained highlight how the optimal resistance-capacity distribution within the external wall turns out different for very heavy, very light and generic walls. In particular, for generic walls, the optimal solution (characterised by the combination of the number of layers to be used and their sequence) can be determined on the basis of an abacus proposed in an original way in this paper. The abacus, drawn for fixed thermal and geometric characteristics of the internal elements and hence knowing the value of complex admittance Λ (in modulus and phase), reports the product $r|\Lambda|$ in ordinates and the product ωrc (ω angular frequency of the outdoor temperature variation) in abscissae. It is divided into a series of regions, each of which corresponds to the set of $\omega rc - r|\Lambda|$ pairs for which the optimal solution is the same, based on the calculations carried out. Consequently, the designer, using the abacus, is able to determine the optimal solution for the external wall for each $\omega rc - r|\Lambda|$ pair. The abacus, if drawn according to the indication of the paper, can constitute an effective support tool for designers in the early design stage when the technical solutions to maximize the thermal resilience of the building are selected.

Declaration of competing interest

The authors declare that they have no known competing financial interests or personal relationships that could have appeared to influence the work reported in this paper.

Data availability

No data was used for the research described in the article.

Appendix 1. Essential details on heat transfer matrix method

Consider an external wall of a building, which separates an internal room from the external environment. The external temperature is assumed to oscillate in time with an angular frequency ω and a period $P=2\pi/\omega$. The internal room temperature will also generate oscillations, exhibiting the same angular frequency and a complex amplitude of the external temperature. In free running behaviour of the building, the internal wall surface complex amplitudes T_{int} (related to the temperature) and q_{int} (related to the heat flux) are linearly linked to the corresponding external wall surface quantities T_{ext} and q_{ext}, as follows:

$$\begin{pmatrix} T_{int} \\ q_{int} \end{pmatrix} = \begin{pmatrix} E & F \\ G & H \end{pmatrix} \times \begin{pmatrix} T_{ext} \\ q_{ext} \end{pmatrix} = Z \begin{pmatrix} T_{ext} \\ q_{ext} \end{pmatrix} \quad (A1.1)$$

where Z represents the wall transfer matrix. In the case of a multi-layered wall consisting of a sequence of N homogeneous layers, the transfer matrix can be evaluated as:

$$Z = Z_{int} \left(\prod_{s=1}^{N} Z_s \right) Z_{ext} \quad (A1.2)$$

where Z_s is the transfer matrix of the generic s-th layer, and Z_{int}, Z_{ext} are defined as:

$$Z_{int} = \begin{pmatrix} 1 & R_{int} \\ 0 & 1 \end{pmatrix}; Z_{ext} = \begin{pmatrix} 1 & R_{ext} \\ 0 & 1 \end{pmatrix}$$

with R_{int} and R_{ext} the internal and external surface thermal resistances respectively.

If x_s, ρ_s, k_s and c_s are the values of thickness (m), density (kg/m^3), thermal conductivity (W/mK) and specific heat at constant pressure (J/kgK) respectively, related to the s-th homogeneous layer (with thermal resistance $R_s = x_s/k_s$ and surface thermal capacity $C_s = \rho_s \bullet x_s \bullet c_s$), the corresponding Z_s matrix elements will be given by

$$E_s = H_s = \cosh((j \cdot \omega \cdot R_s \cdot C_s)^{0.5}); F_s = G_s = R_s^{\,2} \cdot (j \cdot \omega \cdot R_s \cdot C_s)^{-1}$$

Appendix 2. Details on the influence of furnishings

Furnishings can significantly contribute to the room total admittance Λ, and this contribution is usually much more remarkable than that of the room indoor air. We often think, to a first approximation, that the contribution of the furnishings could be included in the term U we find in the Eq. (10). It would involve the above-mentioned objects to be considered as sufficiently thin objects so that their inner conductive resistance could be disregarded (i.e. to be considered as purely capacitive) and the influence of the surface thermal resistances to be disregarded.

In this appendix three furnishings characterized by a simple geometric shape are studied: a slab, a cylinder and a sphere. The admittance λ_0 of each object is calculated, disregarding the inner and outer surface thermal resistances, as ratio between the heat flux coming into the solid and the thermal oscillation on its surface; the effective admittance λ will be then calculated with the Eq. (12).

A SLAB

Let us consider a homogeneous vertical slab to have transversal dimensions much larger than thickness d, and to be lapped by the air on both faces, each of them having area A. What was said in the text with respect to the internal wall delimiting the room can be repeated for each face; it follows that

$$\lambda_0 = \sqrt{j}\,\lambda_\infty \tanh\left(\sqrt{\frac{j}{2}} \cdot \frac{d}{\nu} \right)$$

The weight α will be: α =S*/S ≅ 2A/S, with S* the object's area involved in the thermal transfer.

B. CYILINDER

Let us consider a homogeneous vertical cylinder to have length ℓ being remarkable compared to the radius $\Re$. If an oscillating solution proportional to exp(jωτ) is searched for the temperature, the Fourier equation can be written (in cylindrical coordinates) in the following form:

$$\frac{1}{w} \frac{\partial}{\partial w} \left(w \frac{\partial T}{\partial w} \right) - \frac{j\omega}{\beta} T = 0 \quad (A2.1)$$

with w radial coordinate. Posing, for writing shortness,

$$\psi = \sqrt{\frac{j\omega}{\beta}} = \frac{\sqrt{2j}}{\nu}$$

the general integral in the Eq. (A2.1) can be expressed by the modified Bessel functions $I_0(\psi w)$ and $K_0(\psi w)$ in the form [29]:

$$T = [C_1 I_0(\psi w) + C_2 K_0(\psi w)] \cdot \exp(j\omega\tau)$$

in which, according to the obvious condition that the temperature should remain finite on the symmetry axis, $C_2 = 0$ has to be considered. The inlet flow turns out to be

$$q_e = k \frac{\partial T}{\partial w} = k C_1 \psi I_1(\psi w) \cdot \exp(j\omega\tau)$$

where it was considered that the derivative of the function I_0, compared to its argument, is identical to the function I_1. From the previous relations the following is obtained (the weight α will be: α =S*/S=2π$\Re$ ℓ/S.):

$$\lambda_0 = \left(\frac{q_e}{T}\right)_{w=\Re} = k\psi\frac{I_0(\psi\Re)}{I_1(\psi\Re)} = \sqrt{j}\,\lambda_\infty\frac{I_0\left(\sqrt{\frac{j}{2}}\cdot\frac{\Re}{\nu}\right)}{I_1\left(\sqrt{\frac{j}{2}}\cdot\frac{\Re}{\nu}\right)}$$

c.SPHERE

A homogeneous sphere with radius $\Re$ is being considered. The Fourier equation in spherical coordinates has the following form

$$\frac{1}{w^2}\frac{\partial}{\partial w}\left(w^2\frac{\partial T}{\partial w}\right) - \frac{j\omega}{\beta}T = 0 \tag{A2.2}$$

with w radial coordinate. The general integral of Eq. (A2.2) is [29]:

$$T = \frac{1}{w}[C_1\sinh(\psi w) + C_2\cosh(\psi w)]\cdot\exp(j\omega\tau)$$

where we should have $C_2 = 0$ to assure the T to be finite in the middle of the sphere. The inlet heat flow is given by

$$q_e = k\frac{\partial T}{\partial w} = kC_1\psi I_1(\psi w)\cdot\exp(j\omega\tau)$$

and then

$$\lambda_0 = \left(\frac{q_e}{T}\right)_{w=\Re} = \frac{k}{\Re}\left[\frac{\psi\Re}{\tanh(\psi\Re)} - 1\right] = \frac{\sqrt{j}\,\lambda_\infty}{\tanh\left(\sqrt{\frac{j}{2}}\cdot\frac{\Re}{\nu}\right)} - \frac{k}{\Re}$$

The weight will be $\alpha = S^*/S = 4\pi\Re^2/S$. In this case, in the Eq. (13), an opportune mean value will have to be considered for r_{int}. In any case, when the characteristic dimensions (d and $\Re$) become very large compared to ν, then we shall have $\lambda_0 \to \sqrt{j}\,\lambda_\infty$. If, on the other hand, such dimensions tend to zero, it can be demonstrated that $\lambda_0 \to j\omega m$, where m is the capacity per outer surface unit of the solid under examination; in these conditions, and disregarding the inner and outer surface thermal resistances, the solid under examination can be assimilated to a pure thermal capacity. Obviously, according to the Eq. (12), it does not involve that λ is pure imaginary and, then, that λd can be added to U in the Eq. (10).

Let consider, by way of first example, a low internal partition wall made of Brick-1 (face wall) being 3 m in length, 1,6 m in height and 0,12 m ($S^* \cong 9.60\ m^2$) in thickness. Assuming $r_{int} = 0.13\ m^2$ K/W and P=24 h, $S^*\lambda = 7.95 + 17.34$ J (W K^{-1}) is obtained. By way of second example, let consider a column or a concrete cylindric pilaster being 30 cm in diameter and 3 m ($S^* \cong 2.83\ m^2$) in height; assuming $r_{int} = 0.13\ m^2$ K/W and P=24 h, $S^*\lambda = 9.90 + 7.461$ J (W K^{-1}) is obtained.

References

[1] European Commission. Directive of the European Parliament and of the Council on the energy performance of buildings (recast). Brussels, 2021. Available at: https://eur-lex.europa.eu/resource.html?uri=cellar:c51fe6d1-5da2-11ec-9c6c-01aa75ed71a1.0001.02/DOC_1&format=PDF.

[2] Hafez, F.S., Sa'di, B., Safa-Gamal, M., Taufiq-Yap, Y.H., Alrifaey, M., Seyedmahmoudian, M., Stojcevski, A., Horan, B., Mekhilef, S., 2023. Energy Efficiency in Sustainable Buildings: A Systematic Review with Taxonomy, Challenges, Motivations, Methodological Aspects, Recommendations, and Pathways for Future Research. Energy Strategy Reviews 45, 101013. Doi: 10.1016/j.esr.2022.101013.

[3] F. Belaïd, C. Massié, Driving forward a low-carbon built environment: The impact of energy context and environmental concerns on building renovation, Energy Econ. 124 (2023) 106865, https://doi.org/10.1016/j.eneco.2023.106865.

[4] E. Rodrigues, M.S. Fernandes, A.R. Gaspar, Á. Gomes, J.J. Costa, Thermal transmittance effect on energy consumption of Mediterranean buildings with different thermal mass, Appl. Energy 252 (2019) 113437, https://doi.org/10.1016/j.apenergy.2019.113437.

[5] F. Stazi, G. Ulpiani, M. Pergolini, C. Di Perna, The role of areal heat capacity and decrement factor in case of hyper insulated buildings: An experimental study, Energ. Buildings 176 (2018) 310–324, https://doi.org/10.1016/j.enbuild.2018.07.034.

[6] A. De Gracia, A. Castell, M. Medrano, L.F. Cabeza, Dynamic thermal performance of alveolar brick construction system, Energ. Conver. Manage. 52 (2011) 2495–2500, https://doi.org/10.1016/j.enconman.2011.01.022.

[7] S.B. Sadineni, S. Madala, R.F. Boehm, Passive building energy savings: a review of building envelope components, Renew. Sustain. Energy Rev. 15 (2011) 3617–3631, https://doi.org/10.1016/j.rser.2011.07.014.

[8] B. Xu, X. Xie, G. Pei, New method of equivalent energy consumption for evaluating thermal performance of energy-saving materials in passive buildings, Appl. Therm. Eng. 230 (2023) 120774, https://doi.org/10.1016/j.applthermaleng.2023.120774.

[9] Y. Yang, S. Chen, Thermal insulation solutions for opaque envelope of low-energy buildings: A systematic review of methods and applications, Renew. Sustain. Energy Rev. 167 (2022) 112738, https://doi.org/10.1016/j.rser.2022.112738.

[10] F. Bisegna, B. Mattoni, P. Gori, F. Asdrubali, C. Guattari, L. Evangelisti, S. Sambuco, F. Bianchi, Influence of insulating materials on green building rating system results, Energies 9 (9) (2016) 712, https://doi.org/10.3390/en9090712.

[11] C. Fabiani, A.L. Pisello, Coupling controlled environmental forcing and transient plane source method: an innovative thermal characterization procedure for building insulation materials, Appl. Therm. Eng. 130 (2018) 254–263, https://doi.org/10.1016/j.applthermaleng.2017.10.155.

[12] H. Asan, Numerical computation of time lags and decrement factors for different building materials, Build. Environ. 41 (2006) 615–620, https://doi.org/10.1016/j.buildenv.2005.02.020.

[13] N.C. Balaji, M. Mani, B.V. Venkatarama Reddy, Dynamic thermal performance of conventional and alternative building wall envelopes, J. Build. Eng. 21 (2019) 373–395, https://doi.org/10.1016/j.jobe.2018.11.002.

[14] H. Khaleghi, A. Karatas, Assessing the dynamic thermal performance of prefabricated wall panels in extreme hot weather conditions, J. Build. Eng. 82 (2024) 108351, https://doi.org/10.1016/j.jobe.2023.108351.

[15] M. Ciampi, F. Leccese, G. Tuoni, Multi-layered walls design to optimize building-plant interaction, Int. J. Therm. Sci. 43 (2004) 417–429, https://doi.org/10.1016/j.ijthermalsci.2003.09.006.

[16] G. Barone, A. Buonomano, G.F. Giuzio, A. Palombo, Towards zero energy infrastructure buildings: optimal design of envelope and cooling system, Energy 279 (2023) 128039, https://doi.org/10.1016/j.energy.2023.128039.

[17] F. Leccese, G. Salvadori, F. Asdrubali, P. Gori, Passive thermal behaviour of buildings: performance of external multi-layered walls and influence of internal walls, Appl. Energy 225 (2018) 1078–1089, https://doi.org/10.1016/j.apenergy.2018.05.090.

[18] S. Flores-Larsen, C. Filippín, F. Bre, New metrics for thermal resilience of passive buildings during heat events, Build. Environ. 230 (2023) 109990, https://doi.org/10.1016/j.buildenv.2023.109990.

[19] EN ISO 13786, 2017 (Technical Standard) - Thermal performance of building components. Dynamic thermal characteristics. Calculation methods.

[20] H. Asan, Investigation of wall's optimum insulation position from maximum time lag and minimum decrement factor point of view, Energ. Build. 32 (2000) 197–203, https://doi.org/10.1016/S0378-7788(00)00044-X.

[21] M. Ozel, Thermal performance and optimum insulation thickness of building walls with different structure materials, Appl. Therm. Eng. 31 (2011) 3854–3863, https://doi.org/10.1016/j.applthermaleng.2011.07.033.

[22] M. Ozel, Effect of insulation location on dynamic heat-transfer characteristics of building external walls and optimization of insulation thickness, Energ. Buildings 72 (2014) 288–295, https://doi.org/10.1016/j.enbuild.2013.11.015.
[23] K.J. Kontoleon, T.G. Theodosiou, K.G. Tsikaloudaki, The influence of concrete density and conductivity on walls' thermal inertia parameters under a variety of masonry and insulation placements, Appl. Energy 112 (2013) 325–337, https://doi.org/10.1016/j.apenergy.2013.06.029.
[24] K.J. Kontoleon, C. Giarma, Dynamic thermal response of building material layers in aspect of their moisture content, Appl. Energy 170 (2016) 76–91, https://doi.org/10.1016/j.apenergy.2016.01.106.
[25] P. Gori, L. Evangelisti, C. Guattari, Description of multilayer walls by means of equivalent homogeneous models, Int. Commun. Heat Mass Transfer 91 (2018) 30–39, https://doi.org/10.1016/j.icheatmasstransfer.2017.11.008.
[26] Y. Lu, J. Hu, K. Zhong, Optimization of insulation layer location and distribution considering maximum time lag and damping factor, Case Stud. Therm. Eng. 30 (2022) 101766, https://doi.org/10.1016/j.csite.2022.101766.
[27] Y. Lu, J. Hu, J. Yu, L. Yuan, K. Bao, Analytical solutions for decrement factor and phase shift of wall under periodic fluctuation of outdoor air temperature, Appl. Therm. Eng. 242 (2024) 122487, https://doi.org/10.1016/j.applthermaleng.2024.122487.
[28] S. Wang, Y. Kang, Z. Yang, J. Yu, K. Zhong, Numerical study on dynamic thermal characteristics and optimum configuration of internal walls for intermittently heated rooms with different heating durations, Appl. Therm. Eng. 155 (2019) 437–448, https://doi.org/10.1016/j.applthermaleng.2019.04.005.
[29] H.S. Carslaw, J.C. Jaeger, Conduction of heat in solids. Oxford University Press, 2nd edition, ISBN: 0198533683.
[30] J.H. Lienhard IV, J.H. Lienhard V, A heat transfer textbook (5th edition). Phlogiston Press, Cambridge, USA, 2020.
[31] D. Maillet, S. André, J.C. Batsale, A. Degiovanni, C. Moyne, 2000. Thermal quadrupoles: solving the heat equation through integral transforms. Wiley, Chichester.
[32] F. Fantozzi, P. Galbiati, F. Leccese, G. Salvadori, M. Rocca, Thermal analysis of the building envelope of lightweight temporary housing, J. Phys. Conf. Ser. 547 (2014) 012011, https://doi.org/10.1088/1742-6596/547/1/012011.
[33] D. Mazzeo, G. Oliveti, N. Arcuri, Influence of internal and external boundary conditions on the decrement factor and time lag heat flux of building walls in steady periodic regime, Appl. Energy 164 (2016) 509–531, https://doi.org/10.1016/j.apenergy.2015.11.076.
[34] C. Liu, Z. Zhang, Thermal response of wall implanted with heat pipes: experimental analysis, Renew. Energy 143 (2019) 1687–1697, https://doi.org/10.1016/j.renene.2019.05.123.
[35] Y. Chen, A.K. Athienitis, K.E. Galal, Frequency domain and finite difference modeling of ventilated concrete slabs and comparison with field measurements: Part 2. Application, Int. J. Heat Mass Transf. 66 (2013) 957–966, https://doi.org/10.1016/j.ijheatmasstransfer.2013.07.086.
[36] S. Ginestet, T. Bouache, K. Limam, G. Lindner, Thermal identification of building multilayer walls using reflective Newton algorithm applied to quadrupole modelling, Energ. Build. 60 (2013) 139–145, https://doi.org/10.1016/j.enbuild.2013.01.011.
[37] M.M. Marjanović, R. Gospavić, G. Todorović, An analytical approach based on Green's function to thermal response factors for composite planar structure with experimental validation, Int. J. Therm. Sci. 139 (2019) 129–143, https://doi.org/10.1016/j.ijthermalsci.2019.01.020.
[38] EN ISO 6946, 2017 (Technical Standard) - Building components and building elements. Thermal resistance and thermal transmittance. Calculation methods.
[39] G. Tuoni, Behavior of walls in periodic thermal regime and resonance effects (in Italian), La Termotecnica 1 (1983) 40–48.
[40] M. Ciampi, F. Fantozzi, F. Leccese, G. Tuoni, On the optimization of building envelope thermal performance. Multi-layered walls design to minimize heating and cooling plant intervention in the case of time varying external temperature fields, Civ. Eng. Environ. Syst. 20 (2003) 231–254, https://doi.org/10.1080/1028660031000140224.